

High-temperature oxidation of iridium
by Thomas Leigh George

A thesis submitted in partial fulfillment of the requirements for the degree of MASTER OF SCIENCE in Mechanical Engineering
Montana State University
© Copyright by Thomas Leigh George (1975)

Abstract:
An investigation of the oxidation of iridium wires was conducted in the temperature range of 1965 to 2260 C (2238 to 2533 K). The wires were oxidized in naturally convected CO2 at pressures ranging from 1.32 x 10-3 to 1.32 atm (1 to 1000 torr). The experimental results were compared to values calculated from a model based on the assumptions that the oxidation rate was controlled by the rate of CO2 dissociation, the rate of vaporization of IrO2(g), IrO3(g) and Ir(g) and the rate of the subsequent diffusion of these species through the boundary layer.

STATEMENT OF PERMISSION TO COPY

In presenting this thesis in partial fulfillment of the requirements for the degree of Master of Science in Mechanical Engineering at Montana State University, I agree that the Library shall make it available for inspection. I further agree that permission for extensive copying of this thesis for scholarly purposes may be granted by my major professor, or, in his absence, by the Director of Libraries. It is understood that any copying of publication of this thesis for financial gain shall not be allowed without my written permission.

Thomas L. George
Signature

8/25/75
Date

HIGH-TEMPERATURE OXIDATION OF IRIDIUM

by

THOMAS LEIGH GEORGE

A thesis submitted in partial fulfillment
of the requirements for the degree

of

MASTER OF SCIENCE

in

Mechanical Engineering

Approved:

Albert J. Kumnick
Chairman, Examining Committee

Dennis O. Blackketter
Head, Major Department

Roy L. Hall
for Graduate Dean

MONTANA STATE UNIVERSITY
Bozeman, Montana

August, 1975

ACKNOWLEDGEMENTS

Special thanks and appreciation is due Dr. A.J. Kumnick for his generosity in time and effort throughout the couse of this research project and for serving as head of the associated examining committee. Also to be thanked is Dr. R.T. Wimber for his helpful notes and advice. Thanks are also expressed to Dr. H.W. Townes and Dr. R.L. Mussulman for serving on the graduate committee.

TABLE OF CONTENTS

	Page
VITA	ii
ACKNOWLEDGMENTS	iii
LIST OF TABLES	v
LIST OF FIGURES	vi
ABSTRACT	vii
CHAPTER I. INTRODUCTION	
Characteristics and Uses of Iridium	1
Review of Previous Work	2
Purpose of Present Study	3
CHAPTER II. EXPERIMENTAL PROCEDURE	
Experimental Materials	5
Apparatus and Procedure	5
CHAPTER III. THEORETICAL MODEL	
Modeling Oxidation Rates	10
Theoretical Model for the Rate Oxidation of Iridium	11
CHAPTER IV. RESULTS AND OXYGEN PRESSURE CALCULATIONS	
Experimental Results	20
Calculation of Oxygen Partial Pressure	20
CHAPTER V. DISCUSSION	
Errors in Theoretical Predictions	31
Comment on Free Energies of IrO_2 and IrO_3	32
CHAPTER VI. SUMMARY	36
APPENDIX	37
REFERENCES	46

LIST OF TABLES

Page

TABLE 1 - Values for Unknowns in Rate Equation for CO_2 Dissociations 30

TABLE 2 - Average deviation of Theoretical Equations from Experimental Data 31

TABLE 3 - Comparison of Results Using Linear Free Energy Equations 35

TABLE 4 - Experimental Data 38

LIST OF FIGURES

Page

FIGURE 1 - Schematic Representation of Oxidation Apparatus 6

FIGURE 2 - Typical Rate Plot for an Oxidation Experiment 9

FIGURE 3 - Free Energies of Formation 19

FIGURE 4 - Experimental and Theoretical Results Assuming Local Equilibrium for CO_2 Dissociation 21

FIGURE 5 - Experimental and Theoretical Results Assuming Rate Control for CO_2 Dissociation - Best Fit for All Pressures 22

FIGURE 6 - Experimental and Theoretical Results Assuming Rate Control for CO_2 Dissociation - Best Fit Excluding Highest Pressure 23

FIGURE 7 - Reaction at Gas-Metal Interface 24

ABSTRACT

An investigation of the oxidation of iridium wires was conducted in the temperature range of 1965 to 2260 C (2238 to 2533 K). The wires were oxidized in naturally convected CO_2 at pressures ranging from 1.32×10^{-3} to 1.32 atm (1 to 1000 torr). The experimental results were compared to values calculated from a model based on the assumptions that the oxidation rate was controlled by the rate of CO_2 dissociation, the rate of vaporization of $IrO_2(g)$, $IrO_3(g)$ and $Ir(g)$ and the rate of the subsequent diffusion of these species through the boundary layer.

CHAPTER I

INTRODUCTION

Characteristics and Uses of Iridium

Iridium is considered to be the most corrosion resistant metal known when it is compared with all other metals over a broad range of temperature and in a great variety of corrosive environments [1]. These corrosive environments include numerous acids and salt solutions, molten oxides, fused salts and molten metals.

When iridium is heated in oxygen to about 600 C (873 K) a thin oxide film is produced. At temperatures greater than 1000 C (1273 K) the oxidation products are volatile resulting in an oxidation rate which is constant with time. However, this rate is low enough to allow the use of iridium in contact with oxygen at temperatures above 2000 C (2273 K).

Although iridium has reasonably good high-temeprature strength properties, its high cost limits its use as a structural material. Iridium wires are used as heating elements in high-temperature furnaces and as high-temperature thermocouples. Other possible applications for iridium include coatings for components in rocket engines and leading edges on re-entry spacecraft. Iridium has also been considered as a protective coating for components in high temperature gas cooled nuclear reactors where CO_2 is used as a coolant. The present study is particularly relevant to this consideration.

Review of Previous Work

An extensive reveiw of the literature available on the oxidation of iridium has been presented by Wimber [2] and a brief summary of that review is presented here.

Oxidation studies of iridium carried out by Cordfunke and Meyer [3] indicated IrO_3 as the major oxide specie formed and at temperatures above 1110 C (1383 K) the oxides formed were volatile. Similar results were obtained by Schafer and Heitland [4] and by Alcock and Hooper [5]. Cordfunke and Meyer also arrived at equilibrium constants for the oxidation reaction which were slightly higher than those reported by the other investigators.

A mass spectrometric study by Norman, et al [6] indicated the presence of Ir^+, IrO^+, IrO_2^+, and IrO_3^+ ions during the oxidation of iridium at temperatures between 1557 and 1760 C (1830 and 2033 K). IrO_2 and IrO_3 were found to be the major oxide species. The presence of IrO(g) could not be ruled out, but if it did exist, its partial pressure would be less than 1/50 of the partial pressure of the IrO_2 at the highest temperature and oxygen pressure (10^{-4} atm) involved in the study.

The work of Bartlett [7] on the oxidation of platinum at temperatures greater than 800 C (1073 K) is relevant to the present study because of the chemical similarities between platinum and iridium (Ir is a member of the platinum group) such as the formation of volatile

oxides. Bartlett predicted oxidation rates from calculations involving the reversible reaction, $O_2 + Pt \rightleftarrows PtO_2$, which takes place at the solid-gas interface and the subsequent diffusion of the oxide through the gaseous boundary layer which forms as a result of the natural convection of the oxidizing gas.

Wahl [8] describes two models to predict oxidation rates of iridium wires in air and pure oxygen for both forced and natural convection. One model based on the assumption of diffusion control proved reliable for pressures above 10^{-4} atm. The other model predicted oxidation rates at lower pressures assuming vaporization of the oxide species from the metal surface as the rate limiting process. More recently an equation, similar to that used by Bartlett, was formulated to accommodate both models and produced accurate results for the entire pressure range [9]. The major steps in the derivation of this model are presented in Chapter III.

Purpose of Present Study

The present study attempts to show that the diffusion/vaporization model described above [9] applies to the rate of oxidation of iridium in CO_2, given the amount of oxygen produced by the dissociation of the CO_2.

Several approaches were formulated to predict the available oxygen at the gas-solid interface, none of which proved completely satisfactory.

These included an approach based on the assumption of local equilibrium at the gas-metal interface, an approach assuming kinetic control for the entire dissociation oxidation process, and a model based on kinetic control for the CO_2 dissociation with the major portion of the reaction products being removed by diffusion through the boundary layer.

CHAPTER II

EXPERIMENTAL PROCEDURE

Experimental Materials

The 0.508 mm diameter iridium wire used in this study was commercially pure and from a single lot. Mass spectrometer analysis indicated that the wire was better than 99.8% pure with the major impurities being W (800 ppm), Fe (60 ppm) and Cu (35 ppm).

The CO_2 used was typically 99.99% pure with N_2 the major impurity (20 ppm). Prior to entering the oxidation cell, it was dried first in anhydrous calcium sulfate ($CaSO_4$) and then in magnesium perchlorate ($Mg(ClO_4)_2$).

Apparatus and Procedure

A detailed description of the apparatus and experimental procedure has been given by Wahl [8]. Consequently a more general and brief explanation will be presented here.

A schematic representation of the experimental system is shown in Fig. 1. The iridium wire was mounted between two electrodes in the water-cooled oxidizing cell. The cell was provided with two sight ports covered with rotatable pyrex windows. Through one port an optical pyrometer was focused on the wire and through the opposite window a motor-driven, timer-actuated camera fitted with a telemicroscope was focused on the same point of the wire.

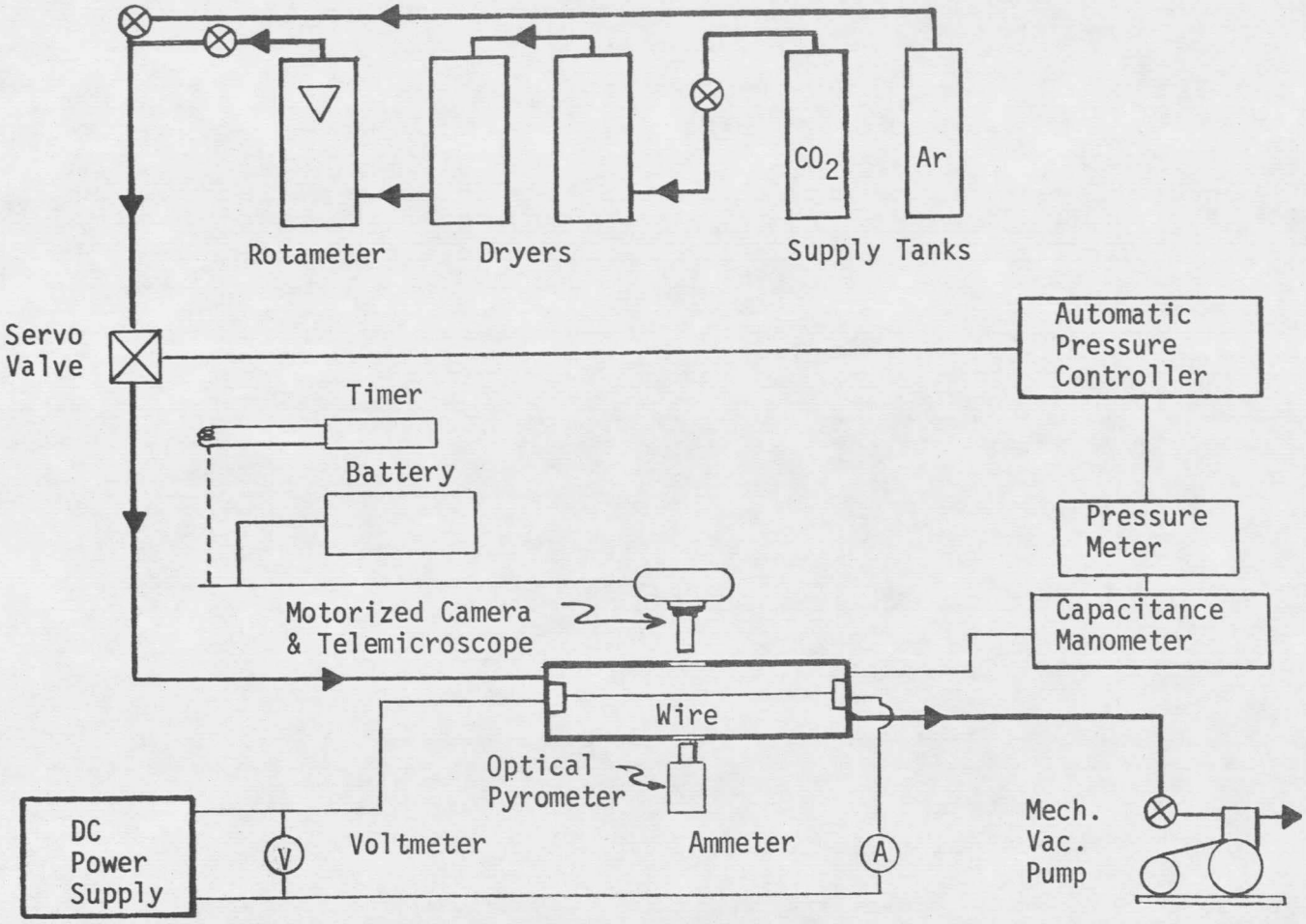


Figure 1: Schematic Representation of Oxidation Apparatus.

The pyrometer was calibrated to compensate for readings taken through the pyrex window as described by Wahl [8]. This calibration was checked periodically throughout the course of the experiments. The wire was maintained at the desired temperature by self-resistance heating. Pressure was held constant at a selected value by use of a servo-controlled valve, coupled with a capacitance monometer. To insure an atmosphere of CO_2 essentially free from oxidation products, a small, constant flow of CO_2 was maintained by continuously operating a vacuum pump connected to the system.

At the beginning of an experimental run a length of iridium wire was cleaned in acetone and mounted between the electrodes in the oxidation cell. The wire was then annealed in an argon atmosphere at 1.05 atm (800 torr) and 2200 C (2437 K) for 30 minutes to prevent excessive recystallization and grain growth from occurring during oxidation measurements. The argon was then pumped out; the cell was then leak-tested and filled with CO_2 to the desired pressure. The servo mechanism was activated and allowed to establish a steady flow. The wire was brought to temperature by adjusting the current from the power supply. The camera-timer system was started and a series of ten exposures was taken of the wire.

The time interval between exposures was set so that approximately 0.025 mm would be removed from the wire diameter during the course of the run. The wire temperature was monitored with the optical pyrometer

and kept constant by current adjustments. On longer runs (up to 48 hours) the system was shut off for periods of time. This procedure was not believed to influence the experimental results because the time required to bring the wire back to temperature was negligible compared to the total elapsed time. Upon completion of the run an exposure was made of a drill rod of known diameter at the same focal length as the wire. This served as a standard for determining the wire diameters. The wire images were measured using a modified cathetometer in which a foil with a 0.05 mm slit was incorporated in the telemicroscope. Using a high-intensity back light on the film and a light meter attached to the eyepiece of the telemicroscope, the image width could be obtained, and converted to a wire diameter using the relationship between the image width of the drill rod and the known drill rod diameter. The repeatability of a single measurement was typically $\pm$0.05 to 0.1 percent. Hills [10] reported that in using this procedure a correction in the diameter measurements must be made due to the appearance of a fringe zone at the edges of the wire image. The thickness of this fringe zone was determined to be a function of the wire temperature and is included in the final calculations for this study.

Typical results of film measurements for a single run are plotted in Fig. 2 where the slope of the line divided by negative two gives the recession rate in cm/sec.

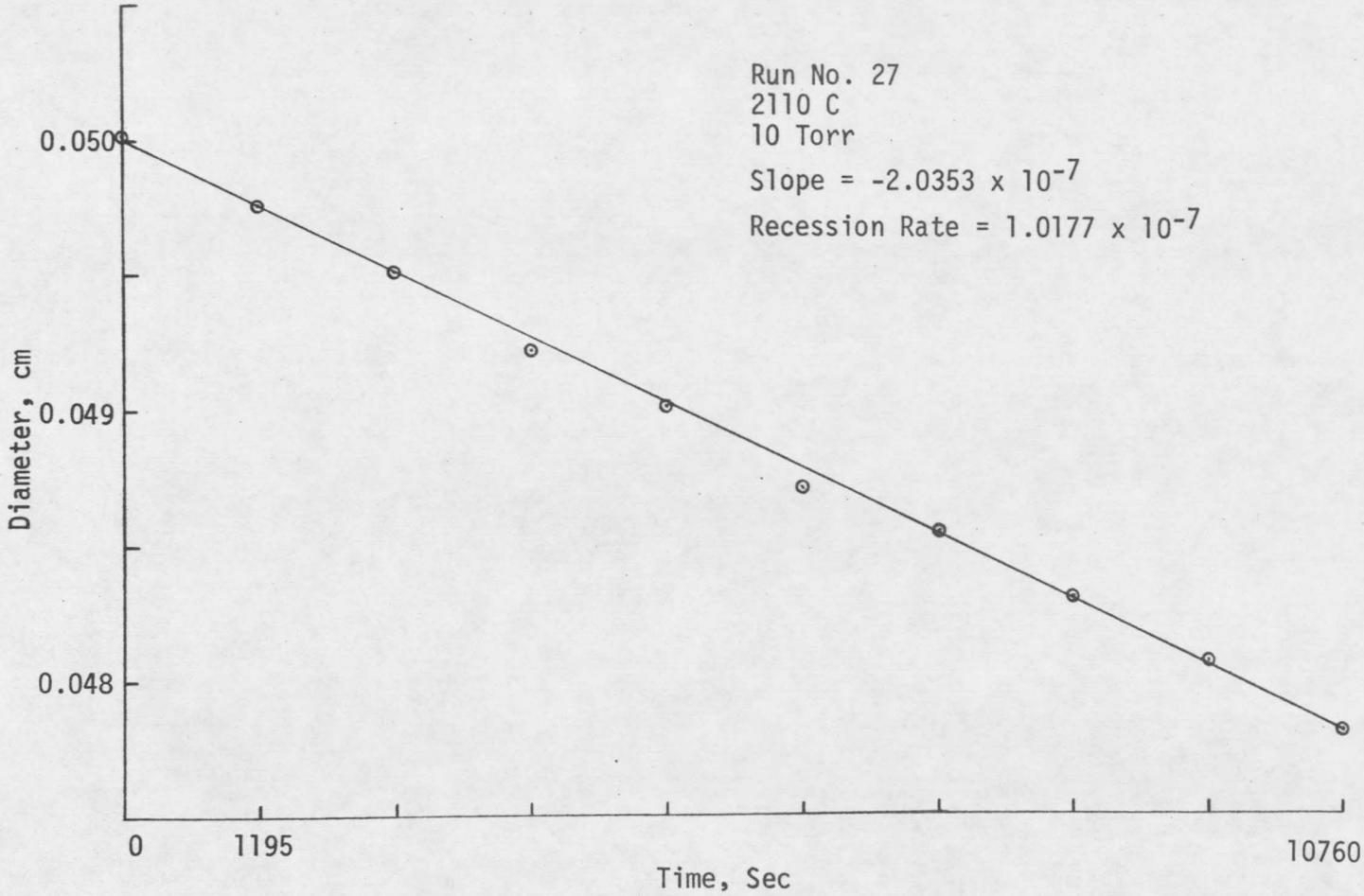


Figure 2: Typical Rate Plot for an Oxidation Experiment.

CHAPTER III

THEORETICAL MODEL

Modeling Oxidation Rates

The term oxidation is used to define the reaction between a metal and oxygen in the absence of water or aqueous phase. The oxidation of most metals is characterized by the build-up of an oxide film on the surface; in many cases (e.g., Al and Cr oxidation) the film acts as a protective coating, while in others (e.g., Fe oxidation) the film is nonprotective. Over a certain temperature range some metals including tungsten, molybdenum, and iridium form oxide species which are volatile. The oxidation of these metals is characterized by a linear rate law.

From an engineering viewpoint, a factor of major interest in the oxidation process is the rate at which it occurs. In formulating a model describing the oxidation process, each step must be considered as potentially rate limiting. Once the limiting step or steps are determined and described quantitatively the rate can be predicted. For the specific case of iridium oxidation in naturally convected CO_2, a reasonable sequence of events based on earlier work is as follows [2]:

1) Oxygen production from CO_2.
2) Adsorbtion of the free oxygen onto the metal surface.
3) Reaction of the oxygen with the solid material on the surface.
4) Desorbtion of the oxide specie or species from the metal surface.

5) Diffusion of the oxides through the boundary layer away from the metal surface.

Theoretical Model for the Rate of Oxidation of Iridium

Wimber, et al [9] formulated a model for the rate of iridium oxidation assuming the vaporization of $IrO_2(g)$, $IrO_3(g)$ and Ir(g) and their subsequent diffusion through the gaseous boundary layer surrounding the material as the controlling step. The model correlated well with experimentally measured recession rates of iridium wires in naturally convected air and oxygen and in forced convection air and oxygen.

As mentioned previously, the model is a synthesis of two separate models, one which held for the higher pressures assuming diffusion of the oxides through the boundary layer as the controlling step, and the other, for the lower pressures, assuming vaporization of the oxide species as the controlling step. The basis for each model and the manner in which they are combined into a single equation are summarized below.

Both models assume each of the oxidation reactions is at equilibrium. Over the temperature and pressure range considered the dominant reactions can be written:

$$Ir + O_{2_S} \overset{K_2}{\rightleftharpoons} IrO_2(g)_S \tag{1}$$

$$Ir + 3/2\ O_{2_S} \overset{K_3}{\rightleftharpoons} IrO_3(g)_S \tag{2}$$

$$Ir \rightleftharpoons Ir(g)_S \tag{3}$$

where the subscript S denotes conditions at the solid boundary, and K_2 and K_3 are equilibrium constants for each reaction.

The oxidation rate is expressed in terms of the recession rate of the surface of the iridium wire. To avoid duplication, the recession rate due to the formation of only one of the oxide species, IrO_2, will be derived. The derivations for the recession rates due to the formation of IrO_3 and Ir(g) are essentially the same.

Equation (1) represents the overall reaction and can be broken down into the process whereby oxygen is adsorbed onto the surface, creating a potential site for the oxidation reaction, and the vaporization of the IrO_2 molecule. Assuming equilibrium between the oxygen and the metal surface, the following reaction equation can be written:

$$|S_2 \overset{k_{2b}}{\underset{k_{2f}}{\rightleftharpoons}} IrO_2(g)_S \tag{4}$$

where $|S_2$ represents the entity at the sites where the vapor specie may form. The net recession rate due to the formation and vaporization of IrO_2 may be expressed as:

$$\dot{X}_{S2} = A(k_{2f}\, C_{S2} - k_{2b}\, P_{2S}) \tag{5}$$

where $\dot{X}_{S2}$ is the surface recession rate with units of length per time, P_{2S} is the partial pressure of $IrO_2(g)$ at the interface, C_{S2} is the concentration of the $|S_2$ entity, A is an equivalent weight (having the units of mass of iridium consumed per mole of oxide species formed) divided by the density of iridium, and k_{2f} and k_{2b} are the forward and reverse reaction rate constants for the reaction given by Eq. (4).

Assuming the forward and reverse reactions as given by Eq. (4) are elementary, allows first order rate equations to be written for each reaction. Solving for k_{2b} in terms of k_{2f} and substituting back into Eq. (5) gives

$$\dot{X}_{S2} = Ak_{2f} C_{S2} [1 - P_{2S}/(K_2 P_{O_2})] \tag{6}$$

where P_{O_2} is the oxygen partial pressure.

The quantity $k_{2f} C_{S2}$ is the vaporization flux and from the Knudsen modification of the Hertz-Langmuir equation [11], the following result is obtained:

$$k_{2f} C_{S2} = K_2 P_{O_2} (2\pi M_2 RT)^{-1/2} \tag{7}$$

where M_2 is the molecular weight of IrO_2, R is the ideal gas constant, and T is the absolute temperature of the metal. Equation (7) gives the flux in moles of vapor molecules per unit area per time and substitution into Eq. (6) yields:

$$\dot{X}_{S2} = AK_2 P_{O_2} (2\pi M_2 RT)^{-1/2} [1 - P_{2S}/(K_2 P_{O_2})] \tag{8}$$

For the diffusion control model, the rate of molecular diffusion through the boundary layer is proportional to the oxide pressure gradient across the boundary layer. Since the experimental apparatus provides a continuous flow of the oxidizing gas through the cell, it is assumed the partial pressure of the oxide species outside of the boundary layer is negligible compared to the partial pressure at the interface; the diffusion flux is then equal to the product of the mass transfer coefficient and the partial pressure at the inner surface of the boundary layer. Thus the recession rate due to the diffusion flux can be expressed by

$$\dot{X}_{D2} = Ak_{G2} P_{2S} \tag{9}$$

where k_{G2} is the mass transfer coefficient for IrO_2.

Assuming negligible rates of reaction between the oxides and the matrix gas allows equating $\dot{X}_{D2}$ to $\dot{X}_{S2}$. Solving for P_{2S} and substituting the results back into Eq. (9) yields the following:

$$\dot{X}_2 = \dot{X}_{D2} = \dot{X}_{S2} = \frac{Ak_{G2} K_2 P_{O_2} (2\pi M_2 RT)^{-1/2}}{k_{G2} + (2\pi M_2 RT)^{-1/2}} \tag{10}$$

where $\dot{X}_2$ is the recession rate due to the formation of IrO_2. Equation (10) should be valid for all pressures. Similar expressions are obtained for $\dot{X}_3$ and $\dot{X}_M$, the recession rates due to the formation of IrO_3 and the vaporization of the iridium metal respectively. Assuming

each of these mass transfer processes operates independently, the total recession rate becomes

$$\dot{X} = \dot{X}_2 + \dot{X}_3 + \dot{X}_M \tag{11}$$

or

$$\dot{X} = A \left[\frac{k_{G2} K_2 P_{O_2} (2\pi M_2 RT)^{-1/2}}{k_{G2} + (2\pi M_2 RT)^{-1/2}} + \frac{k_{G3} K_3 P_{O_2}^{3/2} (2\pi M_3 RT)^{-1/2}}{k_{G3} + (2\pi M_3 RT)^{-1/2}} + \frac{k_{GM} P_M (2\pi M_M RT)^{-1/2}}{k_{GM} + (2\pi M_M RT)^{-1/2}} \right] \tag{12}$$

where the subscript 3 refers to the $IrO_3(g)$ and the subscript M refers to the Ir(g).

Equation (12) was used by Hills [10] to predict recession rates in air and oxygen as a function of temperature and oxygen pressure, and with appropriate modification was applied in the present study to predict recession rates in CO_2.

The mass transfer coefficients for each of the diffusing species in Eq. (12) were calculated using the Chilton-Colburn equations [12]:

$$k_{Gi} = \frac{hP}{RT_f c_p \rho P_{BM}} \left(\frac{c_p \rho D_{vi}}{k} \right)^{2/3} \tag{13}$$

where the subscript i refers to the ith specie, h is the film coefficient for convective heat transfer, P is the total system pressure, c_p is the specific heat of the CO_2, T_f if the absolute film temperature (taken as the average of the wire temperature and the ambient temp-

erature), P_{BM} is the logarithmic mean of the pressures of the CO_2 at the inner and outer edges of the boundary layer, ρ is the density of CO_2, k is the CO_2 thermal conductivity and D_{vi} is the gaseous diffusivity for the ith specie. The CO_2 properties used were valid at the film temperature. The Chilton-Colburn equations used in obtaining Eq. (13) are valid for Prandtl numbers ($c_p\mu/k$, where μ is the CO_2 viscosity) in the range of 0.6 to 100 and Schmidt numbers ($\mu/\rho D_{vi}$) in the range of 0.6 to 2500 [13]. In the present study, the Prandtl numbers ranged from 0.750 to 0.785 and the Schmidt numbers from 0.54 to 1.70. The lowest Schmidt numbers, falling slightly outside the recommended range should not cause serious error in the diffusivities.

The film coefficient, h, was calculated from the Madden-Piret [14] equation for heat transfer from horizontal wires:

$$Nu = \frac{hD}{k} = \frac{2}{C_1(8k\gamma\lambda)/\lambda\mu c_p[\gamma + 1]D) - C_2 \ell n(1 + 2\lambda/D) + C_2\phi} \quad (14)$$

where

$$C_1 = \frac{k_{w,a}}{ak_{w,\lambda}}, \quad C_2 = \frac{k_{w,a}}{k_{\lambda,a}} \quad (15), (16)$$

γ is the CO_2 specific heat ratio, λ is the CO_2 mean free path, D is the wire diameter and α is the thermal accommodation coefficient for energy exchange between the iridium surface and the CO_2. In Eqs. (15) and (16) $k_{w,a}$ is the CO_2 thermal conductivity evaluated at the mean of the temp-

eratures of the wire (subscript w) and the ambient (subscript a). Similar definitions apply to $k_{w,\lambda}$ and $k_{\lambda,a}$ where the λ subscript refers to one mean free path away from the wire. The first two terms in the denominator of Eq. (14) dominate at low pressure whereas, $C_2\phi$ is the dominant term at higher pressures. Wimber [9] experimentally determined ϕ to follow the relationship

$$\phi = \ell n[8.87\ Ra^{-0.354}(T/Ta)^{-0.464}] \qquad (17)$$

where Ra is the Rayleigh number given by

$$Ra = g\rho^2 D^3 \beta c_p[\Delta T]/(\mu k) \qquad (18)$$

where g is the gravitational acceleration, β is the coefficient of expansion for CO_2 (β equals the reciprocal of the absolute temperature for an ideal gas) and ΔT is the temperature difference across the boundary layer.

The gaseous diffusivities, D_{vi}, were calcualted according to the Wilke-Lee modification of the Hirschfelder-Bird-Spotz equation [15] using a value of 33 cc/g-atom [16] for the atomic volume of iridium and a value of 1.92 times the absolute melting temperature of the oxide species for the interaction energy [15].

The partial pressure of iridium metal was calculated from the empirical vapor pressure equation of Honig and Kramer [17]:

$$Log(P_M) = 8464.67/T + 65.5812\ Log(T) - .0100272T + 5.44981T^2 \qquad (19)$$

where P_M is the vapor pressure in torr. CO_2 properties were obtained from the NBS Tables [18] and from Kays [19].

The reaminging 6 unknowns needed to apply Eq. (12) (i.e., C_1, C_2, K_1, K_2, and the oxide melting temperatures) were assumed or fitted to the experimental recession rates using Eq. (12) by Wimber, et al [9].

C_1 and C_2 were expressed as functions of temperature as follows:

$$C_1 = 180.03 - 0.23691T + 1.0005 \times 10^{-4}T^2 - 1.2217 \times 10^{-8}T^3 + 5.4490 \times 10^{-13}T^4 \quad (20)$$

$$C_2 = 1.538 - 5.397 \times 10^{-4}T + 1.366 \times 10^{-7}T^2 \quad (21)$$

The oxide melting temperatures were assigned a common value of 1627 C (1900 K) when it was observed that the overall results were relatively insensitive to the particular temperatures selected.

K_1 and K_2 were evaluated from the free energies of each oxide specie, Eqs. (22), (23).

$$\Delta F_f^\circ[IrO_2(g)] = 11295.16 - 20.50737T + 1.397062 \times 10^{-2}T^2 - 4.220806 \times 10^{-6}T^3 + 4.770036 \times 10^{-10}T^4 \quad (22)$$

$$\Delta F_f^\circ[IrO_3(g)] = -19265.59 + 35.50124T - 2.445677 \times 10^{-2}T^2 + 7.472224 \times 10^{-6}T^3 - 8.539786 \times 10^{-10}T^4 \quad (23)$$

Equations (22) and (23) are plotted in Fig. 3 along with results from other workers [6, 20]. The unexpected shape of these curves will be discussed later (see Chapter V).

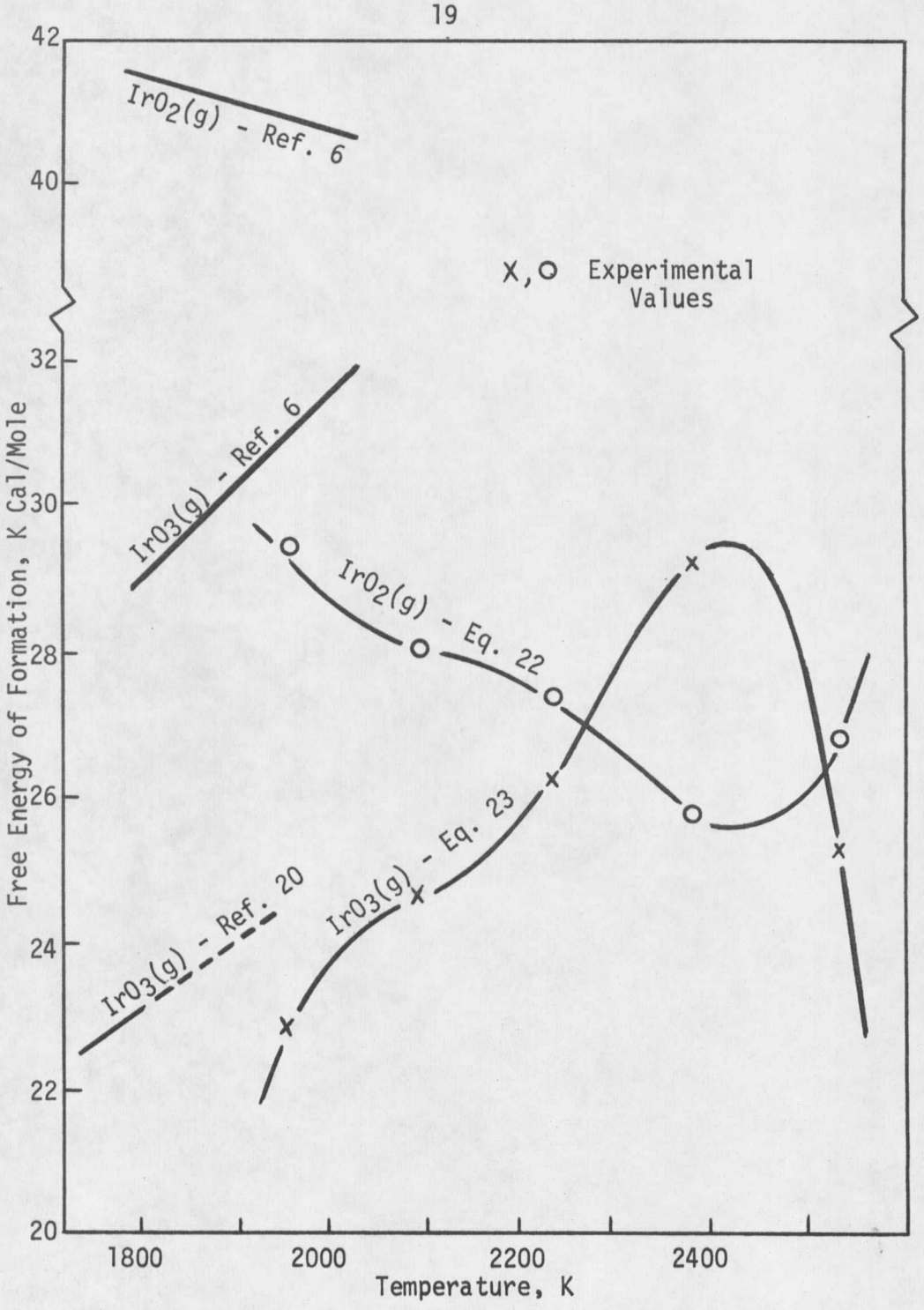


Figure 3: Free Energies of Formation.

CHAPTER IV

RESULTS AND OXYGEN PRESSURE CALCULATIONS

Experimental Results

Experimentally determined recession rates are presented in Figs. 4, 5 and 6 using different symbols to represent data taken at the various temperature levels. The specific temperature and pressure for each data point are given in Table 4 in Appendix A. The solid lines in Figs. 4, 5 and 6 are the results of recession rate calculations using the theoretical model, Eq. (12), and the methods described in the following section to determine the oxygen concentration at the gas-solid interface.

Calculation of Oxygen Partial Pressure

The calculation of recession rates using Eq. (12) requires knowledge of the oxygen partial pressure at the gas-metal interface. In previous work this did not present a problem because the studies were done in oxygen or air where the oxygen partial pressure was immediately given as either the total or a constant fraction of the system pressure.

Oxidation in CO_2 can only occur if CO_2 decomposes and forms oxygen as one of the reaction products. Based on the free energies associated with possible CO_2 reactions virtually all available oxygen was assumed to be produced according to the reaction given by Eq. (24).

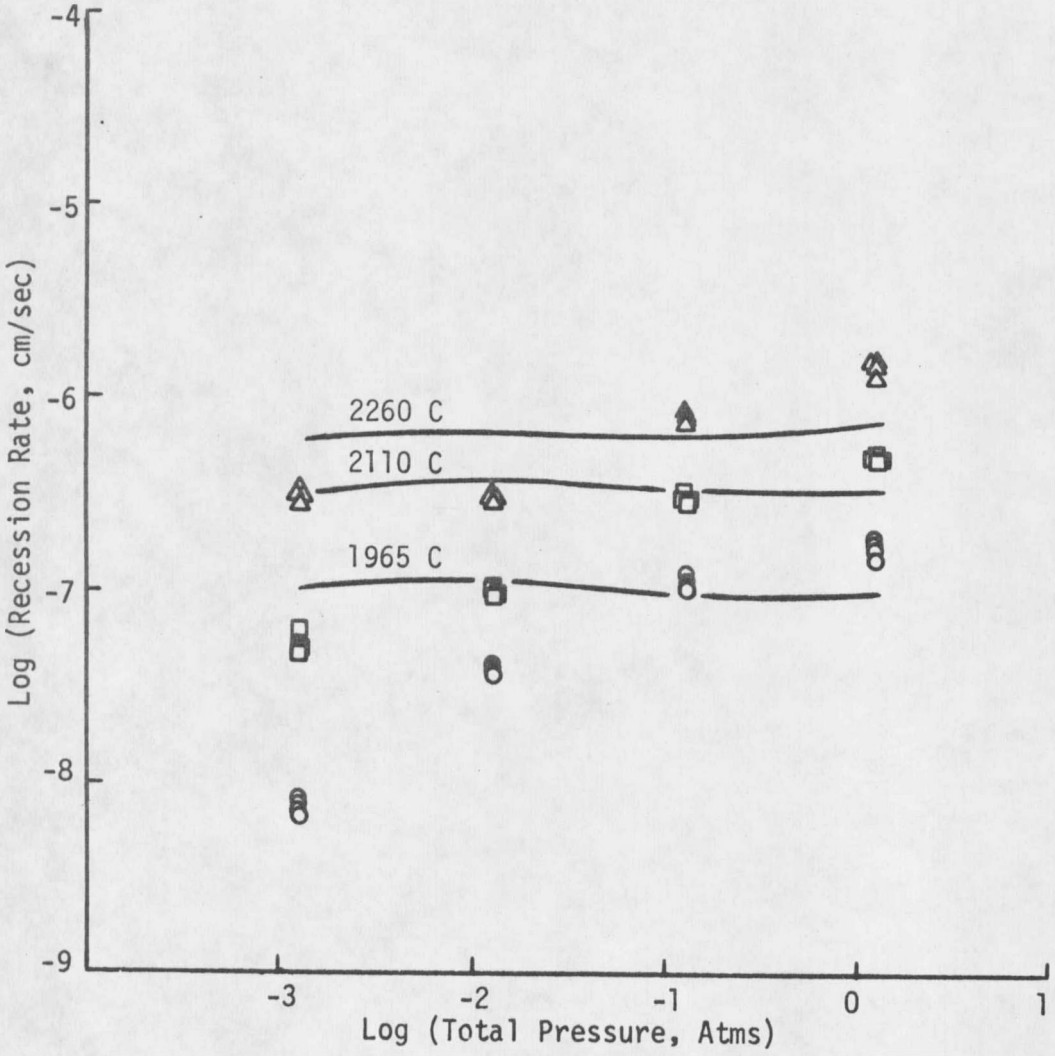


Figure 4: Experimental and Theoretical Results Assuming Local Equilibrium for CO_2 Dissociation.

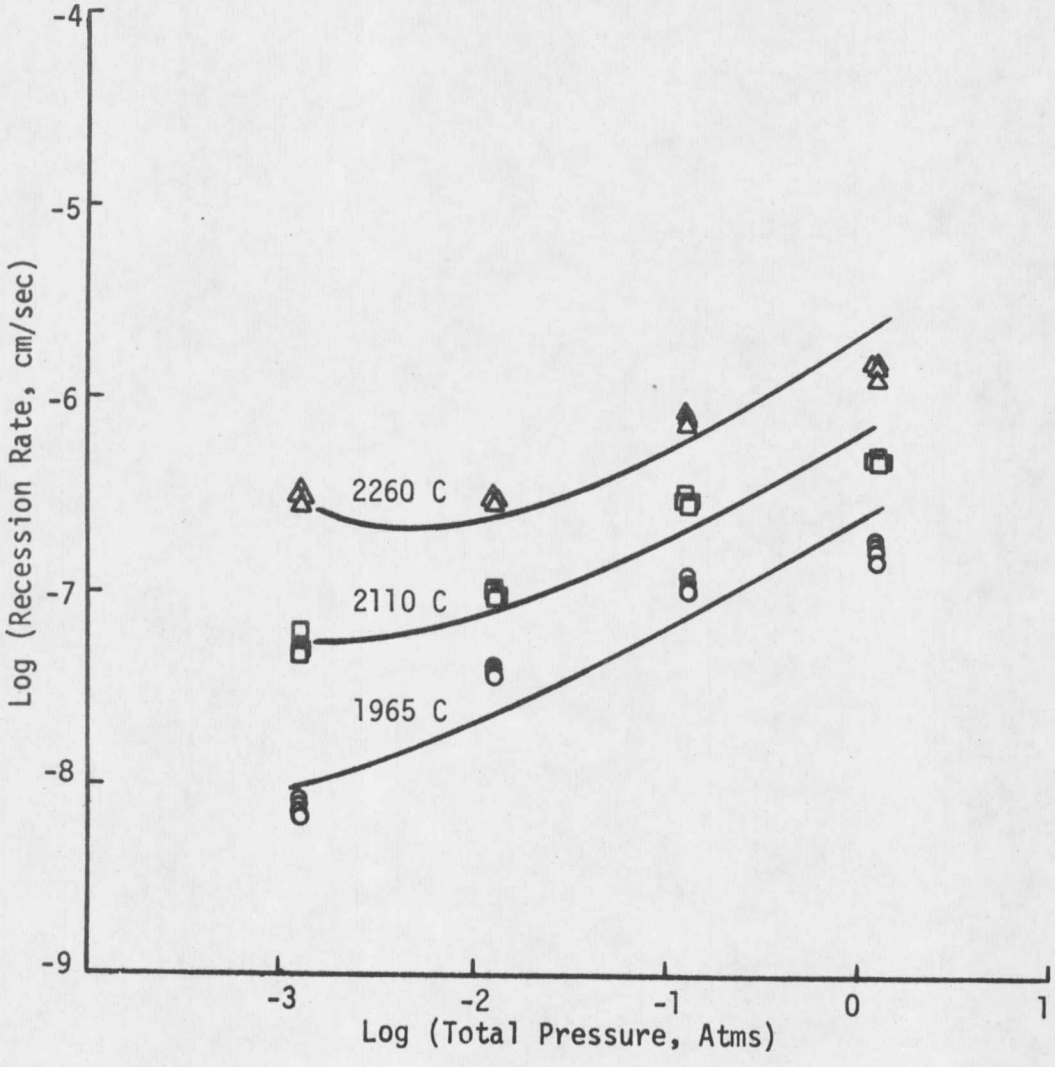


Figure 5: Experimental and Theoretical Results Assuming Rate Control for CO_2 Dissociation. Best Fit for All Pressures.

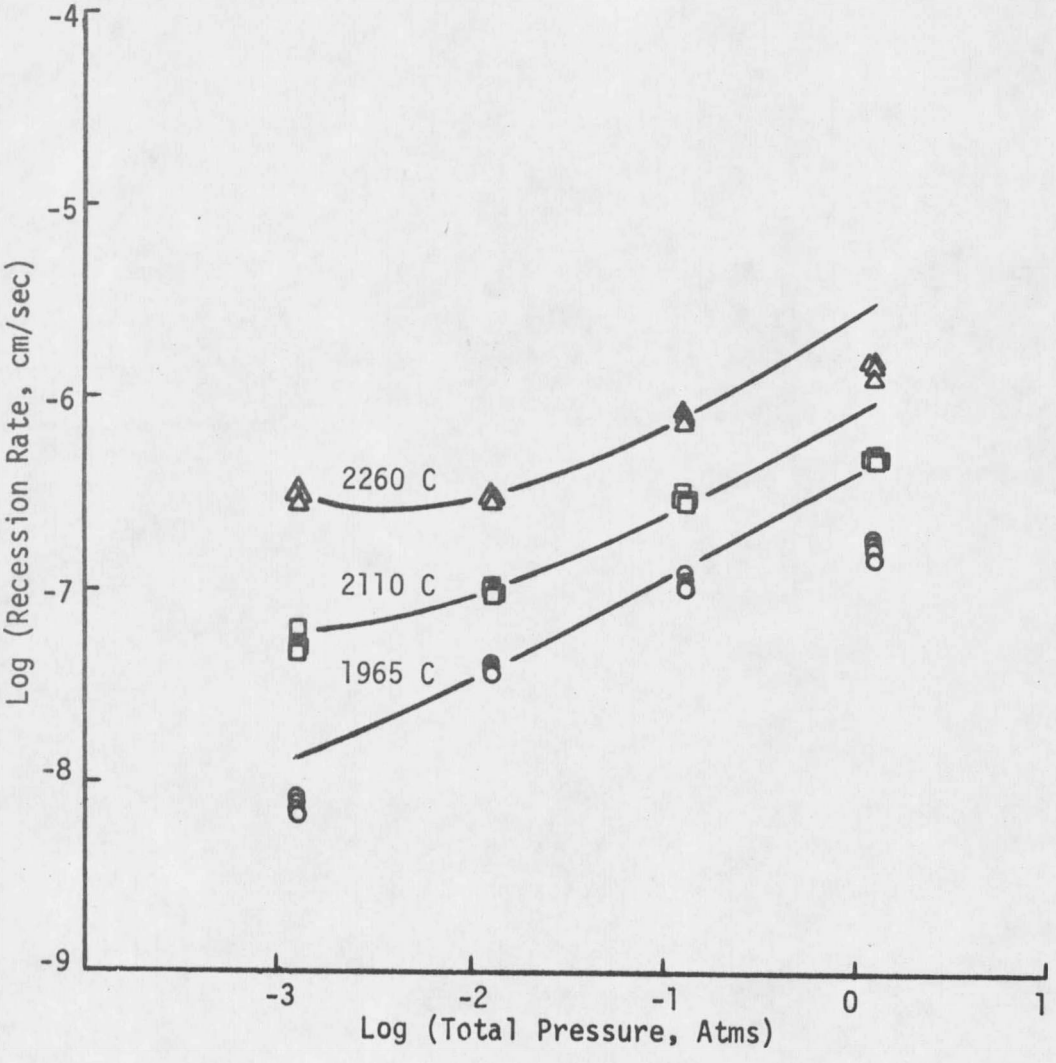


Figure 6: Experimental and Theoretical Results Assuming Rate Control for CO_2 Dissociation. Best Fit Excluding Highest Pressure.

$$2CO_2 \rightleftharpoons 2CO + O_2 \qquad (24)$$

Oxygen partial pressures were calculated for Eq. (24) assuming local equilibrium at the wire surface and using the wire temperature to determine an equilibrium constant. Since the reaction is assumed to take place only in the immediate vicinity of the wire, oxygen may diffuse away from the wire without reacting with the metal. Under steady state conditions the process may be represented as in Fig. 7.

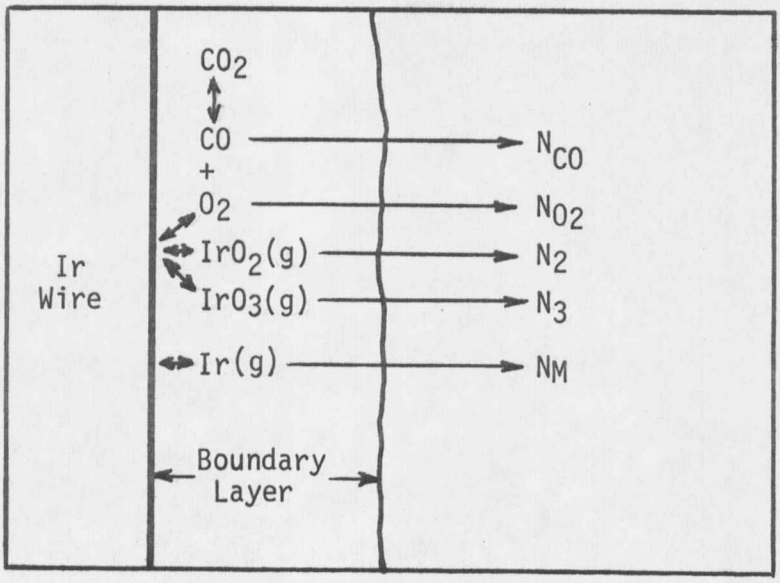


Figure 7: Reactions at Gas-Metal Interface.

where N_{CO}, N_{O_2}, N_2, N_3, and N_M represent the mole flux of each of the species through the boundary layer and each has units of moles per unit area per time. A molecular balance for the oxygen results in the

following relationship:

$$N_{CO} = 2N_{O_2} + 2N_2 + 3N_3 \tag{25}$$

As discussed in Chapter III, Eq. (25) can be written in terms of the partial pressure of each specie at the interface. That is:

$$k_{GCO}P_{CO} = 2k_{GO_2}P_{O_2} + 2k_{G2}P_2 + 3k_{G3}P_3 \tag{26}$$

Considering the total system pressure as the sum of the partial pressures results in

$$P = P_{CO} + P_{O_2} + P_{CO_2} + P_2 + P_3 + P_M \tag{27}$$

where again P_M is the known partial pressure of the vaporized iridium and P is the total system pressure. At equilibrium the dissociation reaction gives the following relationship:

$$K_1 = \frac{P_{O_2} P_{CO}^2}{P_{CO_2}^2} \tag{28}$$

where K_1 is the equilibrium constant and each of the pressures is the partial pressure at the interface. Assuming that each of the oxidation reactions is at equilibrium yields:

$$K_2 = \frac{P_2}{P_{O_2}} \quad \text{and} \quad K_3 = \frac{P_3}{P_{O_2}^{3/2}} \tag{29), (30}$$

The five equations, (26), (27), (28), (29) and (30), in five unknowns, P_{O_2}, P_{CO}, P_{CO_2}, P_2 and P_3, were solved numerically using a

Newton-Raphson iterative scheme. The calculated oxygen partial pressures were substituted in Eq. (12) to give theoretical recession rates which were compared with experimental results. The agreement was not satisfactory; the predicted recession rates exhibited slight CO_2 pressure dependence while experimental recession rates increased significantly with increasing CO_2 pressure as evidenced in Fig. 4. The model's insensitivity to CO_2 pressure is in accord with LeChatelier's principle which implies that for Eq. (24) at fixed temperature, increases in the CO_2 pressure do not result in proportional increases in the oxygen pressure. Since simultaneous diffusion of several gases through a stagnant gas can alter the diffusivities of each, calculations using multicomponent diffusion theory [21] were made to test the magnitude of the effect on the previous result. A change of less than 5% was observed indicating independent diffusion of each gas through the boundary layer was a reasonable assumption for the existing experimental conditions.

The above results suggest the assumption of local equilibirum for the CO_2 dissociation is not valid. Consideration was next directed toward CO_2 dissociation as the rate controlling process. A standard rate control model was not consistent with the observation that at the highest pressure, 1.3 atm (1000 torr), the equilibrium model (Fig. 4) predicted a lower oxidation rate than was observed experimentally.

Since the equilibrium assumption should give an upper bound for the amount of available oxygen, a rate limiting model should predict an even lower oxidation rate and hence not agree with the experimental results. However, the physical aspects of the study (i.e., the dissociation of CO_2 only near an iridium wire) suggest that the wire may assist (other than as a heat source) in the CO_2 dissociation.

One way to take into account the wire's physical presence was to assume that CO_2 molecules dissociated upon hitting the wire with a certain minimum amount of energy which was governed by the molecules' velocity and incident angle of collision. The minimum velocity and allowable incident angle were treated as unknowns to be fitted to the data, using the kinetic gas theory [22] and the Maxwell-Boltzman velocity distribution. An equation for the number of CO_2 molecules striking a unit area of the wire per time with a velocity above the unknown minimum and within the allowable incident angle was derived but comparison with experimental results produced an unsatisfactory fit and the approach was discarded.

Iridium's chemical similarity to platinum suggested a second manner in which the wire may influence the CO_2 dissociation. Since platinum group elements have been known to act as catalysts in several reactions [23], an attempt was made to consider a catalytic type process for the dissociation of CO_2 coupled with diffusion of the reaction products through the boundary layer. The general theory of

catalysis is limited from a quantitative standpoint and furthermore, no specific information for CO_2 on iridium could be found in the literature. In order to simplify the mathematics, the CO_2 dissociation was assumed to be governed by a simple rate equation as shown:

$$R = k(T)[CO_2]^{\sigma} \tag{31}$$

where R is the rate of the reaction in moles/sec, that is, the number of moles of CO_2 which undergo dissociation per second, k(T) is the reaction rate constant, a function of temperature, $[CO_2]$ represents the CO_2 concentration and σ gives the order of the rate law and was assumed constant. Again the situation is as depicted in Fig. 7 with the dissociation reaction going only in the forward direction. It is assumed that the products of this reaction are removed by diffusion through the boundary layer at a rate which is fast enough to allow the dissociation to proceed at a constant rate for a given temperature and pressure. Thus, the mole flux of the CO must be proportional to the rate at which the dissociation reaction proceeds. This can be expressed as

$$N_{CO} = \overline{k}(T)P_{CO_2}^{\sigma} \tag{32}$$

where $\overline{k}(T)$ is the modified rate constant which takes the units necessary to give moles/cm-sec on the left of Eq. (32); the concentration from Eq. (31) is given in terms of the partial pressure of CO_2, which is taken to be the total system pressure.

Once N_{CO} is found Eq. (25) becomes

$$N_{CO} = k_{GO_2} P_{O_2} + k_{G2} P_2 + k_{G3} P_3 \qquad (33)$$

Eq. (33) together with Eqs. (29) and (30) gives 3 equations with 3 unknowns to be solved numerically.

Since no information could be found regarding σ and $\overline{k}(T)$, these were treated as unknowns to be fitted to the data. A simple linear regression was applied to the data from each of the three temperatures individually to find an optimum value for $\overline{k}(T)$ and σ at the temperature. This gave optimum values of σ ranging from 0.44 to 0.48. All the data was then run with σ being stepped through the prescribed range. Optimum $\overline{k}(T)$ values were found for each temperature at each value of σ and the standard deviations calculated. By minimizing the standard deviation, an optimum value of σ was found as well as optimum values for $\overline{k}(T)$. The results which agree reasonably well with the experimental data are presented in Table 1 and Fig. 5.

Although the procedure described above predicted recession rates which were all within a factor of two of the experimental results, the model did not follow the data trend at the highest pressure. The possibility that Eq. (32) does not hold for the highest pressure (see Chapter V) suggested repeating the search for σ and $\overline{k}(T)$ without including the highest pressure data. This resulted in a minor change in σ and more significant changes in the rate constants which had the

effect of shifting the curves upward to give good agreement at least for the three lower pressures. These results are presented in Table 1 and Fig. 6.

TABLE 1

Values for Unknowns in Rate Equation for CO_2 Dissociation

	For Theoretical Results in Fig. 5	For Theoretical Results in Fig. 6
	$\sigma = 0.48$	$\sigma = 0.46$
$\overline{k}$(2260 C)	1.417×10^{-4}	1.698×10^{-4}
$\overline{k}$(2110 C)	6.037×10^{-5}	7.629×10^{-5}
$\overline{k}$(1965 C)	4.035×10^{-5}	6.061×10^{-5}

CHAPTER V

DISCUSSION

Errors in Theoretical Predictions

Average percent errors are given for the two models represented by Figs. 5 and 6 in the table below.

TABLE 2

Average Deviation of Theoretical Equations From Experimental Data

Wire Temp. (°C)	Average Percent Deviation Fig. 5	Fig. 6 (w/o highest press.)
2260	31.5	4.7
2110	27.6	7.9
1965	40.5	27.0

The disparity between the model and the data at the highest pressure is not easily explained because of the many unknown variables involved but two suggestions may be offered. Eq. (31) is valid only at conditions far from equilibrium, and the dissociation reaction may have moved near an equilibrium situation at the highest pressure. As the system pressure is increased, the diffusivities, and hence, the

mass transfer coefficients for all species decrease causing more CO and oxygen to remain at the interface. As the dissociation products build up the reverse reaction rate increases and equilibrium is reached. It is also possible that σ is not pressure independent as was assumed [24].

Figs. 4, 5 and 6 were plotted using an average value for the wire diameter of 0.49 mm. No "standardization" of the wire diameters for the experimental data, as had been done previously [25], was attempted because no strong correlation existed between recession rate and wire diameter.

Comment on Free Energies of IrO_2 and IrO_3

The high-temperature minimum and maximum observed in the plots of the free energies of IrO_2 and IrO_3, Fig. 3, are commented upon by Wimber [9] in the following fashion: "If the minimum and maximum are real, changes in the ΔS_f° values would be associated with reversals in the slopes of the curves and would be difficult to explain". It is suggested by the present author that there may be another set of points (one for each free energy curve) that would be more in keeping with the slopes established by the first four points on each curve but still give satisfactory correlations between the model and the data. Since the curves are fitted to data which represents the sum of the two oxidation reactions, it is conceivable that at the highest temperature this same sum could also be arrived at by using a larger value for

$\Delta F_f°[IrO_3]$ (which would result in less IrO_3 produced) and a correspondingly smaller value for $\Delta F_f°[IrO_2]$ (resulting in more IrO_2 produced). Since the computer program used to optimize the K_2 and K_3 values was not available, a simple test was devised to determine the validity of the above hypothesis. A straight line was fitted through the first four points on each curve and the resulting equations were used to extrapolate free energies at the highest temperature. The new free energy equations are:

$$\Delta F_f°[IrO_2] = 44.979 - 0.0080119T \quad (34)$$

$$\Delta F_f°[IrO_3] = -5.784 + 0.014537T \quad (35)$$

The data to which the free energies, Eqs. (22) and (23), had originally been fitted was still available as was a program which compared this data to recession rates given by Eq. (12). The free energy equations in this program were replaced by Eqs. (34) and (35) and the program run using the old data. The results for some of the highest temperature runs (those for the other temperatures being essentially unchanged) are compared in Table 3. The new equations were not expected to improve the correlation, since in all probability Eqs. (22) and (23) do represent a "best fit", but it was hoped that the correlation would still be reasonable which appears to be the case. The results are even more reasonable when it is considered how sensitive the model is to changes in the free energies. A 10%

change in the free energy for IrO_3 at the highest temperature results in a change greater than 60% in the recession rate due to the formation of IrO_3.

For the present study Eqs. (22) and (23) were used to calculate the free energies. Again, since it is only the sum of the oxidation rates reflected in the data, these equations should work reasonably well to give the correct sum as they seem to have done in the previous studies.

TABLE 3

Comparison of Results Using Linear Free Energy Equations

Run No.	Exp. Rate (cm/s)	Theoretical Rate Using Eqs. (22) & (23)	Theoretical Rate Using Eqs. (34) & (35)
32#	5.25E-07	5.02E-07	5.02E-07
34#	8.11E-07	5.02E-07	5.02E-07
37#	7.17E-07	5.04E-07	5.07E-07
38#	8.39E-07	5.17E-07	5.36E-07
39#	6.73E-07	5.82E-07	6.81E-07
41#	9.34E-07	7.58E-07	1.06E-06
44#	1.60E-06	1.34E-06	1.83E-06
46#	2.24E-06	2.20E-06	2.51E-06
48#	2.82E-06	2.77E-06	3.17E-06
92*	7.36E-07	4.87E-07	4.10E-07
96*	6.47E-07	4.87E-07	4.11E-07
100*	8.40E-07	5.07E-07	4.38E-07
103*	7.43E-07	5.87E-07	5.47E-07
106*	8.38E-07	6.87E-07	6.77E-07
110*	1.42E-06	1.79E-06	2.38E-06
116*	5.55E-06	4.17E-06	6.43E-06
120*	1.26E-05	9.35E-06	1.26E-05
125*	3.43E-05	2.78E-05	2.58E-05
Average Percent Error (Using All Data)		21.0	27.0

# Indicates data from natural convection in air.
* Indicates data from natural convection in oxygen.

CHAPTER VI

SUMMARY

The oxidation rate of the iridium wires in naturally convected CO_2 was assumed to be controlled by three steps:

1) The kineticly controlled production of oxygen from CO_2.
2) The rate of vaporization of the oxide species, $IrO_2(g)$ and $IrO_3(g)$, and Ir(g) from the iridium surface.
3) The rate of diffusion of the oxides and Ir(g) through the boundary layer.

A model was developed to predict the amount of oxygen available for the oxidation reactions at the gas-solid interface. This model was used in conjunction with a previously derived model for the vaporization/diffusion control of iridium oxidation.

Experimental data was collected for iridium wire temperatures of 1965, 2110 and 2260 C (2238, 2383 and 2533 K) in CO_2 atmospheres of 1.32×10^{-3}, 1.32×10^{-2}, 1.32×10^{-1} and 1.32 atm (1, 10, 100 and 1000 torr). The theoretical prediction agreed well with the experimental results for the three lower pressures.

APPENDIX A

TABLE 4

Experimental Data

Run No.	Wire Temp. (C)	Press. (torr)	Wire Diam. (cm)	Experimental Rate (cm/sec)	Calculated Rate (cm/sec)
1	2260	1000	0.0445	1.54E-06	3.13E-06
2			0.0488	1.32E-06	3.14E-06
3			0.0467	1.35E-06	3.13E-06
4			0.0508	1.61E-06	3.14E-06
5		100	0.0443	8.56E-07	7.98E-07
6			0.0494	8.02E-07	7.98E-07
7			0.0465	7.56E-07	7.98E-07
8			0.0445	7.41E-07	7.98E-07
9		10	0.0498	2.88E-07	2.93E-07
10			0.0480	2.86E-07	2.93E-07
11			0.0463	3.09E-07	2.94E-07
12			0.0447	3.05E-07	2.96E-07
13		1	0.0444	2.83E-07	3.25E-07
14			0.0486	3.20E-07	3.16E-07
15			0.0438	3.24E-07	3.26E-07
16			0.0483	3.43E-07	3.17E-07
17	2110	1000	0.0484	4.81E-07	9.20E-07
18			0.0460	5.08E-07	9.19E-07
19			0.0466	4.89E-07	9.20E-07
20			0.0487	4.71E-07	9.20E-07
21		100	0.0492	3.36E-07	2.88E-07
22			0.0479	3.01E-07	2.88E-07
23			0.0459	2.85E-07	2.88E-07
24			0.0427	2.78E-07	2.89E-07
25		10	0.0490	9.50E-08	9.97E-08
26			0.0469	9.75E-08	9.97E-08
27			0.0487	9.38E-08	9.97E-08
28			0.0467	9.79E-08	9.97E-08
29		1	0.0464	4.63E-08	6.06E-08
30			0.0444	6.34E-08	6.11E-08
31			0.0486	4.79E-08	6.00E-08
32			0.0462	5.16E-08	6.06E-08
33	1965	1000	0.0470	1.46E-07	4.27E-07
34			0.0482	1.70E-07	4.28E-07
35			0.0453	1.87E-07	4.27E-07
36			0.0424	1.75E-07	4.26E-07

TABLE 4 (Cont.)

Run No.	Wire Temp. (C)	Press. (torr)	Wire Diam. (cm)	Experimental Rate (cm/sec)	Calculated Rate (cm/sec)
37	1965	100	0.0491	1.09E-07	1.18E-07
38			0.0473	1.03E-07	1.17E-07
39			0.0459	1.23E-07	1.17E-07
40			0.0427	1.11E-07	1.17E-07
41		10	0.0445	3.75E-08	3.65E-08
42			0.0485	4.11E-08	3.66E-08
43			0.0446	4.11E-08	3.66E-08
44			0.0487	3.82E-08	3.67E-08
45		1	0.0493	6.95E-09	1.30E-08
46			0.0465	7.64E-09	1.30E-08
47			0.0490	8.51E-09	1.30E-08
48			0.0476	8.12E-09	1.30E-08

```
C     ::::::::::::::::::::::::::::::::::::::::::::::::::::::::::::::
C
C     THIS PROGRAM CALCULATES RECESSION RATES USING THE
C     COMBINED KINETIC, DIFFUSION CONTROL MODEL AND
C     COMPARES THE RESULTS WITH THE EXPERIMENTAL VALUES
C
C     ::::::::::::::::::::::::::::::::::::::::::::::::::::::::::::::
C
C     VARIABLE LIST
C
C     NCO - CO FLUX THROUGH BOUNDARY LAYER
C     ID2,ID3,ID5,IDM - COLLISION INTEGRALS USED IN CAL-
C     CULATING GASEOUS DIFFUSIVITIES
C     KG2,KG3,KG5,KGM - MASS TRANSFER COEFICIENTS
C     K - THERMAL CONDUCTIVITY OF CO2
C     MU - VISCOSITY OF CO2
C     LAMF - MEAN FREE PATH FOR CO2 MOLECULES
C     M1,M2,M3,M5,MM - MOLECULAR WEIGHTS
C     NUF - NUSSELT NO.
C     G - ACCELERATION DUE TO GRAVITY
C     R - IDEAL GAS CONSTANT
C     TM - MELTING POINT TEMPERATURE FOR OXIDE SPECIES
C     R12,R13,R1M,R15,E12K,E13K,E1MK,E15K - TERMS IN
C                 GASEOUS DIFFUSIVITY COEFS (CF PERRY 4TH ED)
C     JD - WIRE TEMPERATURE INDICATOR
C     PT - SYSTEM PRESSURE IN TORR
C     DIAM - MEASURED WIRE DIAMETER
C     XEXP - EXPERIMENTAL RECESSION RATE
C     RATE - KINETIC REACTION RATE CONSTANT (TEMP DEPENDENT)
C     CP - SPECIFIC HEAT OF CO2
C     GAM - SPECIFIC HEAT RATIO FOR CO2
C     T - WIRE TEMPERATURE (DEG K)
C     P - SYSTEM PRESSURE IN ATM
C     TC - WIRE TEMPERATURE (DEG C)
C     CF - CORRECTION FACTOR FOR WIRE DIAMETER
C     D - CORRECTED WIRE DIAMETER
C     TFK - FILM TEMPERATURE (DEG K)
C     Z2,Z3,ZM - TERMS IN VAPORIZATION FLUX
C     RHO - DENSITY OF CO2
C     V2,V3,V5,VM - TERMS IN GASEOUS DIFFUSIVITIES
C     BETF - COMPRESSIBILITY FACTOR FOR CO2
C     RAF - RAYLEIGH NO.
C     CN,CW - TERMS USED IN CALCULATION OF NUSSELT NO.
C     HC - FILM COEFICIENT
C     DLF2,DLF3 - FREE ENERGIES FOR OXIDES
*
```

```
C       K2,K3 - EQUILIBRIUM CONSTANTS
C       PM - PARTIAL PRESSURE OF IR(G)
C       A -UNITS COEF.
C       ALPHA - EXP IN RATE EQUATION
C       PO2 - PARTIAL PRESSURE OF 02
C       XDOT - CALCULATED RECESSION RATE
C       PERD - PERCENT DEVIATION
        DIMENSION RAT(3)
        REAL NCO
        REAL ID2,ID3,IDM
        REAL ID5,M5,KG5
        REAL K,MU,LAMF,M1,M2,M3,MM,KN,K2,K3,NUF,KG2,KG3,KGM
        F(U)=NCO-2*KG5*P*ALOG(P/(P-U))-2*KG2*K2*U-
       &3*KG3*K3*U**1.5
        F1(U)=-2*KG5*P/(P-U)-2*KG2*K2-3*KG3*K3*1.5*SQRT(U)
        RAT(1)=EXP(-8.681)
        RAT(2)=EXP(-9.481)
        RAT(3)=EXP(-9.711)
        G=980.22
        R=82.056
        M1=44.01
        M2=224.2
        M3=240.2
        MM=192.2
        M5=32
        TM=1900
        R12=4.2895
        R13=4.4455
        R1M=3.8905
        R15=3.7145
        E12K=SQRT(190*1.92*TM)
        E13K=SQRT(190*1.92*TM)
        E1MK=SQRT(190*1.92*2727)
        E15K=144.66
        K=1.9645E-4
        DO 100 JK=1,48
        INPUT JD,PT,DIAM,XEXP
        RATE=RAT(JD)
        GO TO (1,2,3),JD
      1 T=2533;MU=4.9076E-4;CP=.31413;GAM=1.1679;GO TO 4
      2 T=2383;MU=4.7282E-4;CP=.31147;GAM=1.17;GO TO 4
      3 T=2238;MU=4.5528E-4;CP=.30862;GAM=1.1707
      4 P=PT/760
        TC=T-273
*
```

```
      CF=27.2832-.0513385722*TC+3.73412615E-5*TC**2
     &-1.20052194E-8*TC**3+1.43929059E-12*TC**4
      D=CF*DIAM
      XEXP=XEXP*CF*1.E-7
      TFK=(T+281)/2
      Z2=44.3*SQRT(1/M2/T)
      Z3=44.3*SQRT(1/M3/T)
      ZM=44.3*SQRT(1/MM/T)
      RHO=.5363*P/TFK
      LAMF=1.7039E-3*MU*SQRT(TFK)/P
      V2=TFK/E12K
      V3=TFK/E13K
      VM=TFK/E1MK
      V5=TFK/E15K
      ID2=EXP(-.3095824-.567702108*ALOG(V2)+.198735824*
     &(ALOG(V2))**2-.432925677E-1*(ALOG(V2))**3+
     &.357743627E-2*(ALOG(V2))**4)
      ID3=EXP(-.3095824-.567702108*ALOG(V3)+.198735824*
     &(ALOG(V3))**2-.432925677E-1*(ALOG(V3))**3+
     &.357743627E-2*(ALOG(V3))**4)
      IDM=EXP(-.3095824-.567702108*ALOG(VM)+.198735824*
     &(ALOG(VM))**2-.432925677E-1*(ALOG(VM))**3+
     &.357743627E-2*(ALOG(VM))**4)
      ID5=EXP(-.3095824-.567702108*ALOG(V5)+.198735824*
     &(ALOG(V5))**2-.432925677E-1*(ALOG(V5))**3+
     &.357743627E-2*(ALOG(V5))**4)
      DV2=(10.7-2.46*SQRT(1./M1+1./M2))*1.E-4*TFK
     &**1.5*SQRT(1./M1+1./M2)/P/R12**2/ID2
      DV3=(10.7-2.46*SQRT(1./M1+1./M3))*1.E-4*TFK
     &**1.5*SQRT(1./M1+1./M3)/P/R13**2/ID3
      DVM=(10.7-2.46*SQRT(1./M1+1./MM))*1.E-4*TFK
     &**1.5*SQRT(1./M1+1./MM)/P/R1M**2/IDM
      DV5=(10.7-2.46*SQRT(1./M1+1./M5))*1.E-4*TFK
     &**1.5*SQRT(1./M1+1./M5)/P/R15**2/ID5
      BETF=1/TFK
      RAF=G*BETF*RHO**2*(T-281)*D**3*CP/MU/K
      CN=180.0273-2.36913E-1*T+1.000458E-4*T**2-1.221744E-8
     &*T**3
     &-5.449E-13*T**4
      CW=1.538-5.397E-4*T+1.366E-7*T*T
      KN=LAMF/D
      NUF=2/(CN*8*K*GAM*KN/MU/CP/(GAM+1)+CW*ALOG(8.87*
     &RAF**(-.354)*(T/281)**(-.464)/(1+2*KN)))
      HC=NUF*K/D
*
```

```
      KG2=HC*(CP*RHO*DV2/K)**(2./3.)/R/TFK/CP/RHO
      KG3=HC*(CP*RHO*DV3/K)**(2./3.)/R/TFK/CP/RHO
      KGM=HC*(CP*RHO*DVM/K)**(2./3.)/R/TFK/CP/RHO
      KG5=HC*(CP*RHO*DV5/K)**(2./3.)/R/TFK/CP/RHO
      DLF2=11295.155-20.50737*T+.013970621*T*T-4.2208064E-6*
     &T**3+4.770036E-10*T**4
      DLF3=-19265.594+35.501236*T-.024456773*T*T+7.4722242E-
     &6*T**3-8.539788E-10*T**4
      K2=EXP(-DLF2*1000/1.9872/T)
      K3=EXP(-DLF3*1000/1.9872/T)
      PM=(10**(-8464.67/T+65.5812*ALOG10(T)-.0100272*T+
     &5.44981E-7*T**2-200.997))/760
      A=192.2/(22.57/(1.+.664631805E-5*TC-.268733818E-9*TC**
     &2+1.53331753E-12*TC**3-.350592036E-15*TC**4)**3)
      ALPHA=.4601
      NCO=RATE*P**ALPHA
      NL=0
      NN=0
      PO2=.05*P
   31 SAVE=PO2
      IF (NL .GT. 201) OUTPUT 'CANT FIND STARTING POINT',JK;
     &STOP
      IF(PO2 .LT. 0) NL=NL+1;PO2=NL*.005*P;NN=0;GO TO 31
      PO2=PO2-F(PO2)/F1(PO2)
      IF (NN .GT. 20) OUTPUT 'SLOW CONVERGENCE',JK;GO TO 32
      IF (ABS((SAVE-PO2)/SAVE) .GT. .0001) NN=NN+1;GO TO 31
   32 XDOT=A*(KG2*K2*PO2*Z2/(KG2+Z2)+KG3*K3*PO2**1.5*Z3/
     &(KG3+Z3)+KGM*ZM*PM/(KGM+ZM))
      PERD=(XDOT-XEXP)*100/XEXP
      WRITE (108,50) JK,TC,PT,D,XEXP,XDOT,PERD
   50 FORMAT (2X,I4,3X,I5,3X,1PE8.1,3X,0PF7.4,3(3X,1PE10.3))
  100 CONTINUE
      END
C
C     ::::::::::::::::::::::::::::::::::::::::::::::::::::::::::::
*
```

DATA
(UNCORRECTED)

TEMP C	PRESS TORR	DIAM CM	XDOT CM/S
2260	1000	.0468	1.622E-06
2260	1000	.0513	1.383E-06
2260	1000	.0491	1.417E-06
2260	1000	.0534	1.693E-06
2260	100	.0465	8.991E-07
2260	100	.0519	8.429E-07
2260	100	.0489	7.942E-07
2260	100	.0468	7.792E-07
2260	10	.0518	3.026E-07
2260	10	.0504	3.008E-07
2260	10	.0487	3.250E-07
2260	10	.0470	3.208E-07
2260	1	.0466	2.973E-07
2260	1	.0511	3.360E-07
2260	1	.0461	3.404E-07
2260	1	.0507	3.603E-07
2110	1000	.0505	5.019E-07
2110	1000	.0480	5.304E-07
2110	1000	.0486	5.104E-07
2110	1000	.0509	4.912E-07
2110	100	.0514	3.506E-07
2110	100	.0499	3.202E-07
2110	100	.0479	2.974E-07
2110	100	.0446	2.896E-07
2110	10	.0512	9.914E-08
2110	10	.0489	1.018E-07
2110	10	.0509	9.791E-08
2110	10	.0487	1.022E-07
2110	1	.0484	4.836E-08
2110	1	.0463	6.613E-08
2110	1	.0507	4.997E-08
2110	1	.0482	5.381E-08

1965	1000	.0491	1.527E-07
1965	1000	.0504	1.774E-07
1965	1000	.0473	1.949E-07
1965	1000	.0443	1.825E-07
1965	100	.0513	1.138E-07
1965	100	.0494	1.072E-07
1965	100	.0479	1.290E-07
1965	100	.0446	1.161E-07
1965	10	.0465	3.921E-08
1965	10	.0507	3.888E-08
1965	10	.0465	4.298E-08
1965	10	.0509	3.989E-08
1965	1	.0515	7.263E-09
1965	1	.0485	7.984E-09
1965	1	.0512	8.891E-09
1965	1	.0498	8.481E-09

::::::::::::::::::::::::::::::::::::

REFERENCES

1. Anon., Iridium, The Metal, Its Alloys, Chemical Compounds and Catalytic Properties, The International Nickel Co., New York, N.Y., 1965.

2. R.T. Wimber, High-Temperature Oxidation of Iridium, First Annual Progress Report, RLO-2228-T1-1, February, 1971.

3. E.H.P. Cordfunke and G. Meyer, "The System Iridium-Oxygen, I. Measurements of the Volatile Oxide of Iridium", Rec. Trav. Chim., 81, pp. 495-504, 1962.

4. V.H. Schafer and H.J. Heitland, "Gleichgewichtsmessungen im System Iridium-Sauerstoff Gasformiges Iridiumtroxyd", Z. Anorg. Allgem. Chem., 304, pp. 249-65, 1960.

5. C.B. Alcock and G.W. Hooper, "Thermodynamics of the Gaseous Oxides of the Platinum-Group Metals", Royal Society of London, Proceeding Series A, 254, pp. 551-61, 1960.

6. J.H. Norman, et al, "Mass Spectrometric Study of Gaseous Oxides of Iridium", Journal of Physical Chemistry, 42, pp. 1123-4, 1965.

7. R.W. Bartlett, "Platinum Oxidation Kinetics with Convective Diffusion and Surface Reaction", J. Electrochem. Soc., 114(6), 547-550, 1967

8. N.K Wahl, Natural-Convection High-Temperature Oxidation of Iridium, Master's Thesis, Montana State University, June, 1974.

9. R.T. Wimber, et al, "Kinetics of Evaporation/Oxidation of Iridium", To be published in Met. Trans.

10. S.W. Hills, High-Temperature Oxidation of Iridium, Master's Thesis, Montana State University, December, 1974.

11. A.W. Searcy, D.V. Ragone, and U. Colombo, Chemical and Mechanical Behavior of Inorganic Materials, pp. 108-110, Wiley-Interscience, New York, 1970.

12. T.K. Sherwood and R.L. Pigford, Absorption and Extraction, 2nd ed., pp. 52-92, McGraw-Hill, N.Y., 1952.

13. J.R. Welty, C.E. Wicks, and R.E. Wilson, Fundamentals of Momentum, Heat, and Mass Transfer, p. 551, J. Wiley and Sons, New York, 1969.

14. A.J. Madden, Jr. and E.L. Piret, Proceedings of the General Discussion on Heat Transfer, pp. 328-33, IME and ASME, New York, 1951.

15. R.E. Emmert and R.L. Pigford, Chemical Engineers Handbook, 4th ed., Sect. 14, pp. 20-21, Mcgraw-Hill, New York, 1963.

16. R.T. Wimber and H.G. Kraus, "Oxidation of Iridium", Met. Trans., 5, pp. 1565-72, 1974.

17. R. Honig and D.A. Kramer, Techniques of Metals Research, Vol IV, Part I, pp. 515-16, John Wiley and Sons, New York, 1970.

18. J. Hilsenrath, et al, Tables of Thermal Properties of Gases, NBS Circ. 564, 1955.

19. W.M. Kays, Convective Heat and Mass Transfer, p. 359, McGraw-Hill, New York, 1966.

20. A. Olivei, "Methods for Studying Oxygen-Platinum Metals Interaction", Journal of the Less Common Metals, 29, pp. 11-23, 1972.

21. J.O. Hirschfelder, R.B. Bird, and E.L. Spotz, "Viscosity and Other Physical Properties of Gases and Gas Mixtures", Trans. of ASME, p. 934, November, 1949.

22. R.D. Present, Kinetic Theory of Gases, pp. 12-80, McGraw-Hill, New York, 1958.

23. P.H. Emmet, Catalysis, Vol. I, pp. 119-95, Reinhold Publishing Corp., 1954.

24. G.B. Skinner, Introduction to Chemical Kinetics, p. 9, Academic Press, New York, 1974.

25. H.G. Kraus, Natural Convection, High Temperature Oxidation of Iridium, Master's Thesis, Montana State University, June, 1973.

MONTANA STATE UNIVERSITY LIBRARIES
3 1762 10013808 8

N378
G294
cop.2

George, Thomas L
High-temperature oxidation of iridium

DATE	ISSUED TO

N378
G294
cop. 2